Membrane Protein Topology: Amino Acid Residues in a Putative Transmembrane α-Helix of Bacteriorhodopsin Labeled with the Hydrophobic Carbene-Generating Reagent 3-(Trifluoromethyl)-3-(*m*-[^{125}I]iodophenyl)diazirine†

Josef Brunner,* Alexis J. Franzusoff,‡ Bernhard Lüscher,§ Carmen Zugliani, and Giorgio Semenza
Laboratorium für Biochemie, Eidgenössische Technische Hochschule, ETH-Zentrum, CH-8092 Zürich, Switzerland
Received February 26, 1985

ABSTRACT: Labeling of integral proteins with 3-(trifluoromethyl)-3-(*m*-[^{125}I]iodophenyl)diazirine ([^{125}I]TID) was shown previously [Hoppe, J., Brunner, J., & Jørgensen, B. B. (1984) *Biochemistry 23*, 5610–5616] to be affected strongly by interactions among membrane-embedded polypeptide segments. This study describes a detailed analysis of the [^{125}I]TID-label distribution pattern among individual amino acids in a membranous segment of bacteriorhodopsin (bR) following its labeling in purple membrane. The segment analyzed (residues 84–99 in the bR amino acid sequence) is predominantly hydrophobic and has been suggested to be part of the third transmembrane α-helix in the bR polypeptide chain. Within this segment eight residues were identified to be labeled by [^{125}I]TID. Their distribution along the polypeptide chain is consistent with the idea that in the native protein this segment forms a helix whose cylindrical envelope is accessible to the labeling reagent from one face only. Thus, the labeling pattern suggests a possible correlation between lipid contact of individual residues and their labeling by [^{125}I]TID. The finding that [^{125}I]TID labeling occurred at the less polar half of the helix surface (assuming 3.6 residues per turn of the coil) is further consistent with the view that bR is an "inside-out" protein with the majority of polar and charged residues facing the interior of the molecule and nonpolar residues exposed to the lipid bilayer [Engelman, D. M., & Zaccai, G. (1980) *Proc. Natl. Acad. Sci. U.S.A. 77*, 5894–5898].

Labeling of the hydrophobic core of membranes with photoactivatable reagents is a rapid and convenient technique to identify those segments of integral proteins that are embedded in the lipid bilayer (Klip & Gitler, 1974; Chakrabarti & Khorana, 1975; Bercovici & Gitler, 1978; Bayley & Knowles, 1978a,b; Brunner & Richards, 1980; Brunner & Semenza, 1981). Among the various categories of reagents, those containing the diazirino function are particularly attractive because of their favorable chemical and photochemical properties (Bayley & Knowles, 1978b; Gupta et al., 1979; Brunner, 1981; Bayley, 1983).

Recent work involving Edman degradations of membranous polypeptide segments of F_0 subunits from F_1F_0 ATP synthase (*Escherichia coli*) labeled with 3-(trifluoromethyl)-3-(*m*-[^{125}I]iodophenyl)diazirine ([^{125}I]TID)[1] supports the view that the carbene generated from [^{125}I]TID is capable of reacting with most if not all of the amino acid side chains, including aliphatic residues (Hoppe et al., 1984). Furthermore, from analyses of the distributions of radiolabel that resulted upon labeling of the proteins in the presence and in the absence of $NaDodSO_4$ (which is known to affect interactions between membranous segments), it was concluded that labeling patterns of proteins are largely determined by the accessibility of the reagent to individual polypeptide segments and amino acids. An interesting feature of the labeling patterns was the occurrence of polypeptide segments within which the label was distributed in a periodic manner with an average of three to four residues between predominantly labeled sites. These patterns have been interpreted to suggest helical structures of the respective segments, which due to protein–protein interactions were accessible to the reagent from one side only. Label distribution patterns showing similar periodicities have more recently been found also in two other proteins, the c subunit of F_1F_0 ATP synthase from *Neurospora crassa* (Hoppe & Sebald, 1984) and the light-harvesting protein of chromatophores from *Rhodospirillum rubrum* (unpublished experiments). If, as suggested, [^{125}I]TID labeling patterns can indeed be correlated with structural and topological features of proteins, it is obvious that this and related reagents have considerable potential for mapping the protein–lipid interface of integral proteins. Moreover, unlike other carbene generators used for photolabeling (diazo ketones, diazo esters), diazirines are highly susceptible to photolysis, thus permitting reagent activations within the subsecond or submillisecond range. Therefore, photolabeling of membranes with diazirines also represents a potentially powerful tool for the investigation of processes that are accompanied by time-dependent changes in the exposure of protein surface areas to the lipid bilayer. Examples are the insertion into and the translocation of proteins across membranes.

In view of these potentialities, we decided to further investigate the performance of [^{125}I]TID by evaluating the label distribution pattern resulting from [^{125}I]TID labeling of one of the best characterized proteins, bacteriorhodopsin (bR). This light-driven proton pump of *Halobacterium halobium* has an M_r of 27 788, and its polypeptide chain has been proposed to cross the membrane 7 times via predominantly α-

† This work was supported by the Swiss National Science Foundation, Bern, and Hoffmann-La Roche, Basel.
‡ Present address: European Molecular Biology Laboratory, D-6900 Heidelberg, FRG.
§ Present address: Institut für Molekularbiologie II der Universität Zürich, Hönggerberg, CH-8093 Zürich, Switzerland.

[1] Abbreviations: TID, 3-(trifluoromethyl)-3-(*m*-iodophenyl)diazirine; bR, bacteriorhodopsin; HPLC, high-performance liquid chromatography; TLC, thin-layer chromatography; TFA, trifluoroacetic acid; CNBr, cyanogen bromide; $NaDodSO_4$, sodium dodecyl sulfate; PAGE, polyacrylamide gel electrophoresis; AEAP, 3-[(2-aminoethyl)amino]propyl; PTH, phenylthiohydantoin; DMF, dimethylformamide.

0006-2960/85/0424-5422$01.50/0

helical rods (Henderson & Unwin, 1975). On the basis of the electron density map of purple membrane, all of the helical rods of bR show extensive contact with neighboring helices, and most or all of them seem to be partially exposed to the lipid bilayer. Such structural features of bR should result in label distribution patterns of transmembrane helical segments that are similar to those mentioned above, i.e., showing periodicities that reflect the number of amino acid residues per turn of the helical polypeptide chain. For reasons to be explained, the present analysis was focused on one particular helical segment, the third in the sequence. This paper describes a detailed analysis of the label distribution pattern within this segment and provides further suggestive evidence that [^{125}I]TID-labeling patterns of integral proteins can be correlated with lipid–protein contact.

Experimental Procedures

Reagents. [^{125}I]TID was prepared according to published procedures with a specific radioactivity of 10 Ci mmol^{-1} (Brunner & Semenza, 1981; Brunner et al., 1983). It was stored at −20 °C as an ethanolic solution (30–50 mCi mL^{-1}) and used within 2 weeks of preparation. All other chemicals and solvents were commercial grades and, when not further specified, of highest purity.

Purple Membranes. H. halobium (strain S-9) cells were grown and purple membranes prepared according to published procedures (Oesterhelt & Stöckenius, 1974). For preparation of [*Leu*-^{14}C]bacteriorhodopsin, cells were grown under normal conditions to nearly the end of exponential growth phase and the initiation of bR formation, as measured by the absorbance at 560 nm (Oesterhelt & Stöckenius, 1974). Subsequently, the cells were sedimented and resuspended in a synthetic medium in which a mixture of amino acids substituted for the peptone. The mixture of amino acids was as described by Engelman & Zaccai (1980) except it contained only trace quantities in Leu present as [^{14}C]Leu (approximately 1 mCi/4 L of culture medium). Cell growth was then continued until no further production of bR was measurable. Isolation of the purple membranes was then performed as described (Oesterhelt & Stöckenius, 1974).

[^{125}I]TID Binding to Purple Membranes. The (physical) partitioning of [^{125}I]TID into purple membranes was determined from measurements of [^{125}I]TID concentrations before and after sedimentation of membranes that had been equilibrated with the reagent (total [^{125}I]TID concentrations 2×10^{-8} M, 5×10^{-6} M, 2.5×10^{-5} M, 5×10^{-5} M, and 10^{-4} M). The partition coefficient P_L [defined as in Brunner & Semenza (1981)] was calculated on the basis of a 4:1 (w/w) protein:lipid ratio in purple membranes (Stöckenius, 1980).

[^{125}I]TID Labeling of Purple Membranes. For [^{125}I]TID activation, the photolysis apparatus described earlier was used (Brunner & Semenza, 1981). Samples of purple membranes (0.12 mg of protein/mL) in 10 mM Tris-HCl–0.1 M NaCl, pH 7.4, were first deoxygenated by flushing with N_2 for 5 min. Subsequently, 0.1–0.5 mCi of [^{125}I]TID was added (final ethanol concentration less than 1%), and the membranes were equilibrated for additional 10 min at 30 °C. Activation of the reagent (90 s) took place in a thermostated (30 °C) quartz cell. Labeled membranes were collected by sedimentation (60 min, 40000*g*).

Delipidation of Bacteriorhodopsin. For delipidation of bR, 10–20 mg of unlabeled or [^{125}I]TID-labeled purple membranes was dissolved in approximately 2 mL of HCOOH (100%) and the deeply orange solution diluted with ethanol to a final HCOOH:ethanol ratio of 1:2.8 (v/v). Separation of protein and lipid was accomplished by gel filtration on Sephadex LH-60 (3 × 30 cm), which had been equilibrated and eluted with the above-mentioned solvent mixture. Fractions containing protein (recognized by their intense color) were pooled and evaporated to dryness on a rotary evaporator (20 °C). Traces of ethanol were removed by dissolving the residue in 1–2 mL of formic acid and reevaporating the solvent.

Cyanogen Bromide Degradation of Bacteriorhodopsin. Delipidated protein was dissolved in 100% HCOOH and then diluted with water to 70% HCOOH (10 mg of protein/mL). Approximately 5.4 mg of CNBr was added per milligram of protein, and then the solution was incubated in the dark for 48 h (under N_2). Solvent and excess of CNBr were removed by rotary evaporation (30 °C).

Separation of Cyanogen Bromide Fragments of Bacteriorhodopsin. CNBr peptides of bR were separated according to size by Sephadex LH-60 gel filtration on a 2.5 × 60 cm column with HCOOH–ethanol (1:2.8 v/v) as the eluant. The flow rate was approximately 20 mL h^{-1}. Protein eluted was monitored (A_{280nm}), and fractions of approximately 5 mL were collected. Fractions containing peptides of interest were pooled and evaporated to dryness.

Purification of CNBr 9a by Reverse-Phase HPLC. The pool of peptides containing CNBr 9a was dissolved in 100% HCOOH and subjected to reverse-phase HPLC (LiChrosorb RP-18, 5-μm particles, 4.5 × 250 mm). Solvent A was H_2O–HCOOH (9:1 v/v); solvent B was ethanol–HCOOH (9:1 v/v). Two to three milligrams of peptide (dissolved in 0.4 mL of 100% HCOOH) was injected at 50% solvent B, and the column was developed as shown in Figure 2 (see Results). Fractions containing CNBr 9a were pooled and rotary evaporated, the residue was dissolved in 0.5 mL of HCOOH, diluted with 10 mL of water, and lyophilized. The yield was approximately 2.5 mg of pure CNBr 9a (white powder), starting from 20 mg of bR.

NaDodSO$_4$–PAGE of CNBr Fragments of Bacteriorhodopsin. This was carried out in 15% polyacrylamide slab gels (1-mm thick) containing 0.1% NaDodSO$_4$, 6 M urea, and 0.1 M sodium phosphate, pH 7.2 (Shapiro et al., 1967). Peptide samples were dissolved in 10 mM sodium phosphate, pH 7.2, 7 M urea, 1% NaDodSO$_4$, 1% β-mercaptoethanol, and 0.01% bromophenol blue and incubated for 5 min at 95 °C. The gels were fixed, stained, and destained as described by Lämmli (1970).

Solid-Phase Edman Degradation of CNBr 9a and [^{125}I]-TID-Labeled CNBr 9a. (A) Homoserine Lactone Activation. Lyophilized CNBr 9a (1–2 mg) was transferred into a glass test tube, dissolved in 1 mL of TFA, and kept at 25 °C for 1 h. TFA was then evaporated in a desiccator over KOH and the activated peptide dried in vacuo (10^{-2} mmHg) for 5 min.

(B) Peptide Coupling to Controlled Pore Glass. Homoserine lactone activated CNBr 9a (1–2 mg) was dissolved in DMF (freshly distilled over P_2O_5, 0.3 mL/mg of peptide) and the solution reacted with AEAP-glass (prepared by treatment of CPG/100 with a 2% (w/v) solution of [3-[(2-aminoethyl)amino]propyl]trimethoxysilane in acetone, 100 mg of AEAP-glass/mg of peptide) in the presence of *N*-methylmorpholine (freshly distilled over ninhydrin, 30 μL/mg of peptide) at 45 °C for 3 h (slow rotation). Following this coupling step, the glass beads were filtered on a small sintered glass funnel and washed with DMF (2 mL), methanol (3 × 1 mL), HCOOH (3 × 1 mL), methanol (3 × 1 mL), 1,2-dichloroethane (3 × 1 mL), and ether (3 × 1 mL). The glass was dried in vacuo.

(C) Trypsin Cleavage of CNBr 9a Coupled to Glass. A total of 100 mg of glass containing CNBr 9a was suspended

in 0.4 mL of 50 mM NH_4HCO_3 and treated with 20 μL of a solution of trypsin (3 mg mL^{-1} in the same buffer) for 3 h at 37 °C. Following filtration, the glass was washed with water, methanol, formic acid (80%), methanol, and ether and then dried in vacuo.

(D) Automated Solid-Phase Edman Degradation of CNBr 9a Treated with Trypsin. The glass-coupled peptide was subjected to Edman degradation by the automated solid-phase sequencing method in a Sequemat Mini 15 model. Sequencing was performed at 49 °C with 0.4 M *N*-methylmorpholine/TFA, pH 8.1, in pyridine–water (3:2 v/v) as the coupling buffer and methanol and 1,2-dichloroethane as the washing solvents. Coupling reaction was performed for 12 min with 10% PITC (60 μL min^{-1}) and coupling buffer (120 μL min^{-1}); washing was performed with methanol (8 min, 1 mL min^{-1}), 1,2-dichloroethane (2 min, 1 mL min^{-1}), methanol (4 min, 1 mL min^{-1}), and 1,2-dichloroethane (2 min, 1 mL min^{-1}). TFA cleavage was performed for 20 min (70 μL min^{-1}), but TFA was collected only between minutes 4 and 20. Following cyclization, the column was washed again with methanol (5 min, 1 mL min^{-1}) and coupling buffer (4 min, 120 μL min^{-1}). Thiazolinones thus obtained in 1.1 mL of TFA were dried for 30 min at 65 °C in vacuo. The conversion into and analysis of PTH-amino acid derivatives were done as described by Hoppe & Sebald (1980) and Hoppe et al. (1984).

Synthesis of 2,2,2-Trifluoro-1-phenylethyl Propionate. A dispersion of 2,2,2-trifluoroacetophenone (10 mmol) and 2.5 mmol of $LiAlH_4$ was refluxed in ether for 1 h and subsequently quenched with 3 M H_2SO_4. Extraction with ether gave the 2,2,2-trifluoro-1-phenylethanol, which was then propionylated with propionyl chloride in pyridine as described previously for the acetyl derivative (Peters et al., 1968). The crude product was purified by column chromatography (silica gel 60) with ether–hexane (1:2 v/v) as the eluant. Upon evaporation of the solvent, the colorless oily residue was subjected to a bulb to bulb distillation. TLC (ether/hexane, 1:2 v/v) showed a spot at R_f 0.65; the infrared spectrum showed a strong band at 1760 cm^{-1}, which is due to the ester carbonyl. Anal. Calcd for $C_{11}H_{11}F_3O_2$: C, 56.90; H, 4.77. Found: C, 56.15; H, 4.68.

Measurements of the Stability of 2,2,2-Trifluoro-1-phenylethyl Propionate. At time zero, 20 mL of the ester was dissolved either in 1 mL of ethanol–formic acid (2.8:1 v/v) or in 0.5 mL of 1.5 M methanolic HCl. After desired incubation times (at room temperature), aliquots of 10 mL (formic acid–ethanol system) or 2 μL (methanolic HCl system) were diluted with methanol to approximately 80 μL and injected into a reverse-phase HPLC column (LiChrosorb RP-18, 5 μm particles, 4.5 × 250 mm) that had been equilibrated with 50% aqueous methanol. With a flow rate of 2 mL min^{-1}, the column was then developed by linearly increasing the methanol concentration (50%–100% within 15 min), and the components eluted were monitored by their UV (254 nm) absorbance. Under these conditions, 2,2,2-trifluoro-1-phenylethanol and 2,2,2-trifluoro-1-phenylethyl propionate were eluted as well separated peaks at approximately 73% and 92% methanol, respectively. Relative concentrations of either component were established from the UV absorbance signals recorded.

Results

Partitioning of [^{125}I]TID into Purple Membranes. The concentration dependence of the distribution of [^{125}I]TID between the aqueous phase and purple membrane was determined by following sedimentation of the membranes that had been equilibrated with the reagent. At 0.12 mg of protein/mL and total [^{125}I]TID concentrations between 2×10^{-8} and 10^{-4} M, the fraction of reagent that partitioned and sedimented with the membranes was nearly constant (range 76%–82%). This corresponds to a partition coefficient P_L of approximately 1.7×10^5. Within the range of reagent concentrations examined, we could not detect changes in the spectral properties of bR, demonstrating that the reagent does not induce major structural or conformational changes in bR. It can be estimated that at the highest [^{125}I]TID concentration examined (10^{-4} M), the amount of reagent bound to the purple membrane corresponds to nearly that of the endogeneous phospholipids. Thus, these data revealed a remarkably high capacity of purple membrane to bind [^{125}I]TID and they further indicate that the reagent interacts nonspecifically by simply partitioning into the hydrophobic phase of the membrane.

Photoactivated Labeling of Bacteriorhodopsin with [^{125}I]-TID. To further investigate the interactions of [^{125}I]TID with bR, purple membranes (0.12 mg of protein mL^{-1}), equilibrated with [^{125}I]TID at concentrations from 2×10^{-8} to 10^{-4} M, were irradiated for 90 s (this period of time was shown to be sufficient for essentially complete photolysis of the diazirine). Following separation of protein from noncovalently bound radiolabel by gel filtration, the extent of [^{125}I]TID labeling of bR was determined. At all [^{125}I]TID concentrations examined, we found almost identical extents of labeling (5.7%–6.3% of the radiolabel originally introduced). Thus, this result further supports the view (see above) that the interaction of [^{125}I]TID with bR is nonspecific (no saturable sites) and does not induce major changes in the conformation of bR and shows that the distribution of [^{125}I]TID radiolabel within the bR polypeptide chain is largely independent of the concentration of reagent in the lipid phase.

CNBr 9a Contains a Transmembrane α-Helix Suitable for Subsequent Analysis of [^{125}I]TID-Labeling Patterns: General Considerations to Its Isolation. In spite of considerable efforts made to correlate segments of the bR sequence to positions in the electron-density map, these assignments are still tentative. Recent work by Engelman's group suggests that helix C (the third transmembrane helix in the sequence) is in either position 6 or position 7 in the structural map (Trewhella et al., 1983), implying that it is one of those helices that have their axes nearly perpendicular to the plane of the bilayer. Since we expected more easily interpretable labeling patterns from such a helix, the present investigation was focused on a bR segment containing (most of) helix C (residues 80–100 in the bR sequence). On the basis of previous fragmentation data (Khorana et al., 1979), we have decided to choose a CNBr fragment, CNBr 9a according to the nomenclature of Gerber & Khorana (1982), for the present analysis. CNBr 9a comprises residues 69–118 of the bR molecule. As shown before (Khorana et al., 1979), when immobilized to glass via its C terminus, it can be further cleaved with trypsin to yield a glass-bound fragment comprising residues 83–118 of bR.

Unlike the c subunit of F_1F_0 ATP synthases from *E. coli* (Hoppe et al., 1984) and *N. crassa* (Hoppe & Sebald, 1984) or glycophorin A (Ross et al., 1982) and cytochrome b_5 (Takagaki et al., 1983a,b), of which sites of photolabeling have also been determined, bR is a protein that has a considerable mass embedded in the lipid bilayer. It was already clear at the outset that Edman sequencing of [^{125}I]TID-labeled CNBr 9a (or its tryptic fragment) would require preceding separation, purification, and identification of photolabeled hydrophobic peptides. By considering that photolabeling of a protein with an extremely reactive carbene is nonstoichiometric and occurs at a large number of sites, the purification and identification of [^{125}I]TID-labeled CNBr 9a was expected to represent a

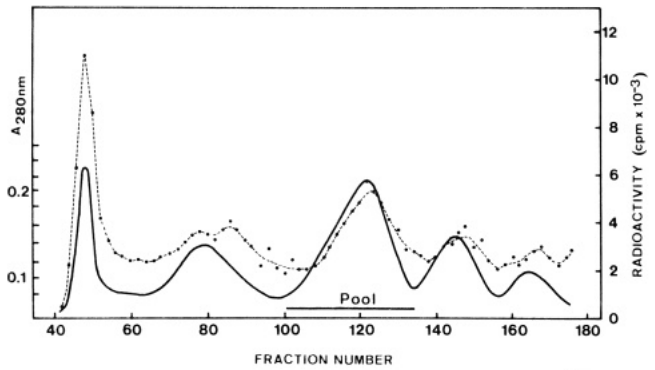

FIGURE 1: Cyanogen bromide cleavage of bR labeled with [^{125}I]TID in purple membrane. Labeled and delipidated (see text) protein (20 mg) was dissolved in 2 mL of 70% (v/v) formic acid and treated with CNBr (5.4 mg/mg of protein; 48 h at room temperature). Following evaporation of the solvent and excess CNBr, the residue wad dissolved in 2 mL of anhydrous formic acid and diluted with 5.6 mL of ethanol, and the clear solution obtained was applied to a Sephadex LH-60 column (2.5 × 60 cm) that had been equilibrated with formic acid–ethanol (1:2.8 v/v). Elution of the protein fragments was performed with the same solvent; the flow rate was approximately 20 mL h^{-1}. Peptides eluted were monitored by their absorbance at 280 nm (—) and the radioactivity associated (●) was determined in individual fractions collected.

major difficulty in the present work. In fact, such difficulties have recently been described for the purification of the membrane-spanning tryptic peptides of the α-polypeptide from Na,K-ATPase labeled with another carbene-generating reagent, 1-tritiospiro[adamantane-4,3′-diazirine] (Nicholas, 1984). Following Khorana's methdology for isolating hydrophobic bR fragments, we also attempted to purify CNBr 9a by a combination of gel filtration (Sephadex LH-60) in ethanol–formic acid and reverse-phase HPLC.

Separation of CNBr Fragments of [^{125}I]TID-Labeled bR by Gel Filtration. Following [^{125}I]TID labeling of purple membrane, deplipidation, and CNBr fragmentation of bR, the resulting polypeptides were subjected to Sephadex LH-60 gel filtration. Figure 1 demonstrates that the positions of the major protein and radioactivity elution peaks are similar, indicating that most of the fragments contain radiolabel. This was further substantiated by NaDodSO$_4$–PAGE with subsequent autoradiography of the dried slab gels (data not shown). Among the CNBr fragments of bR, only CNBr 6 and CNBr 9a [nomenclature of Gerber & Khorana (1982)] have so far been identified in our laboratory. All of CNBr 9a is eluted within fractions 100–135 (Figure 1); however, this pool also contains a fraction of CNBr 6 as well as other hitherto not identified fragments. In spite of the differences shown in Figure 1 in the distribution of radioactivity and absorbance at 280 nm over the elution profile, the urea–NaDodSO$_4$–polyacrylamide gel electrophoretic patterns of individual peptide samples did *not* reveal a different elution behavior of the unlabeled (visualized by Coomassie blue) and [^{125}I]TID-labeled (visualized by autoradiography) CNBr fragments. Thus, this result is in agreement with a similar finding by Nicholas (1984) and confirms the usefulness of Sephadex LH-60 gel filtration for the fractionation according to size of photolabeled hydrophobic peptides.

Purification of [^{125}I]TID-Labeled CNBr 9a. Final purification of [^{125}I]TID-labeled (and unlabeled) CNBr 9a was achieved by reverse-phase HPLC essentially as described by Khorana's group (Gerber et al., 1979). On the basis of the radioactivity elution profiles and urea–NaDodSO$_4$–polyacrylamide gel electrophoretic analyses, [^{125}I]TID-labeled CNBr 9a was eluted within two, overlapping peaks (Figures

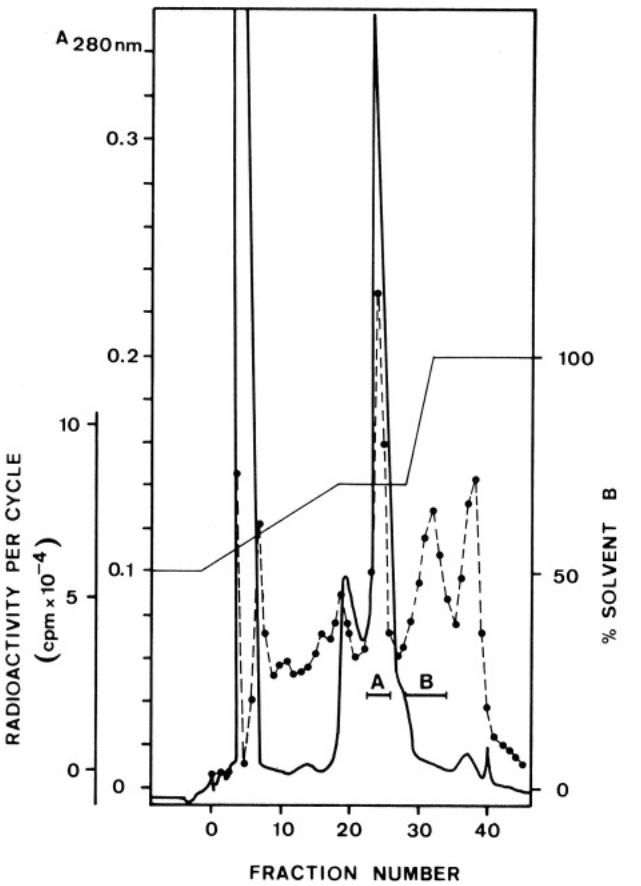

FIGURE 2: Purification of [^{125}I]TID-labeled CNBr 9a. The solution of labeled peptides (pool of fractions 100–135 in the elution diagram shown in Figure 1) was evaporated to dryness, and the residue was dissolved in 100% formic acid. The sample was then subjected to reverse-phase HPLC (see Experimental Procedures) with the solvent gradient indicated. The flow rate was 2 mL min^{-1}. Peptides eluted were monitored by their UV absorbance at 280 nm (—), and the radioactivity in each fraction (1 mL) collected was determined (●).

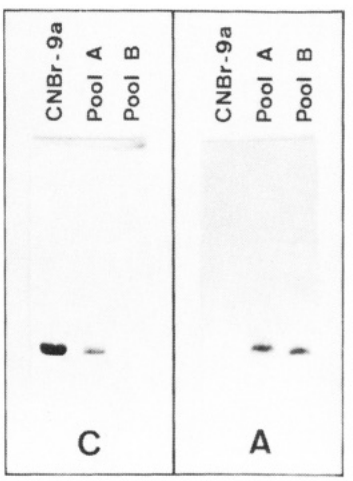

FIGURE 3: NaDodSO$_4$–urea–polyacrylamide gel electrophoretic analysis of [^{125}I]TID-labeled CNBr 9a purified by reverse-phase HPLC. Peptide samples ($\leq$10 μg of peptide) were electrophoresed and proteins stained with Coomassie blue. The destained and dried gel was then subjected to autoradiography with a Kodak X-0-mat film. The peptide samples examined were authentic CNBr 9a (lane 1), peptide from pool A (see text) (lane 2), and peptide from pool B (see text) (lane 3). The left half of the figure (C) shows the Coomassie blue stained gel; the right half (A), the corresponding autoradiogram.

2 and 3). One of these peaks has a shape and position indistinguishable from that of the unlabeled CNBr 9a (A_{280nm})

whereas the second one has a broad asymmetric shape and appeared at an increased content of solvent B. This suggests that [^{125}I]TID-labeled CNBr 9a consists of a variety of molecular species that differ in hydrophobicity, the main parameter on which reverse-phase chromatography is based.

Unambiguous identification of the radiolabled peptides eluted with peaks A and B (Figure 2) was difficult because the [^{125}I]TID-labeled species constitute only a minor fraction of the total CNBr 9a present (trace labeling). However, when samples of the individual peaks were subjected to urea–NaDodSO$_4$–polyacrylamide gel electrophoresis, the radioactive peptides (visualized by autoradiography of the dried gel) had electrophoretic mobilities identical with to that of CNBr 9a (Figure 3). Further evidence that the two peaks contained [^{125}I]TID-labeled CNBr 9a will be presented below.

Identification of Amino Acids in CNBr 9a Labeled by [^{125}I]TID. CNBr 9a consists of 50 amino acid residues (residues 69–118 in the bR sequence), and the putative [^{125}I]TID-labeled stretch (helix C) starts at around residue 11 (Tyr$_{79}$ in bR) (Trewhella et al., 1983). Identification of the [^{125}I]TID-labeled sites was based on solid-phase Edman degradation of that segment. For coupling and sequencing, [^{125}I]TID-labeled CNBr 9a was either used as collected from HPLC (pool A) or diluted with unlabeled CNBr 9a (pool B). In either case the fraction of actually labeled material was less than 5%.

Prior to sequencing, the peptide immobilized to glass was treated with trypsin, a procedure that had been shown previously (Khorana et al., 1979) to liberate an N-terminal 14-residue peptide. In bR, this segment is assumed to be mostly exposed to the aqueous phase (Trewhella et al., 1983). With this step, the number of necessary Edman degradation cycles could be reduced, and the reliability increased in the assignment of radiolabel to individual residues.

(A) Coupling of [^{125}I]TID-Labeled CNBr 9a to AEAP-Glass. Under the experimental conditions used, coupling yields of 43 ± 3% (SD, n = 4) were obtained for [^{14}C]Leu-labeled CNBr 9a. Essentially identical values were also obtained for [^{125}I]TID-labeled CNBr 9a species both from pool A and pool B. This suggests that homoserine lactone activation and coupling to glass was not affected by the [^{125}I]TID labeling of the peptide.

(B) Trypsin Cleavage. This cleavage occurred nearly to completion (>90%) as concluded from sequencing of the remaining peptide and quantitative analyses of the PTH-amino acids. Trypsin treatment of the [^{125}I]TID-labeled glass-immobilized CNBr 9a liberated approximately one-fifth (range 17%–24%) of the radioactivity originally bound to glass, implying that this fraction of the radioactivity was associated with the predominantly hydrophilic segment cleaved off. In a control experiment with [^{14}C]Leu-labeled CNBr 9a, we measured an equal fraction of radiolabel released during the trypsin cleavage step. Since the peptide liberated does not contain Leu and metabolic interconversion of Leu into other amino acids was negligible (shown by the ^{14}C radioactivity profile obtained from sequencing of the peptide still bound to glass), we must assume that the trypsin treatment and subsequent washing procedure caused some hydrolysis of the peptide–glass linkage. From this experiment, we can rule out the possibility that substantial [^{125}I]TID labeling took place within the hydrophilic portion of CNBr 9a.

(C) Edman Degradation. This was performed on the trypsin-treated fragment of [^{125}I]TID-labeled CNBr 9a from both pool A and pool B. Figure 4 shows the profiles of radioactivity released at each degradation cycle. The distinct

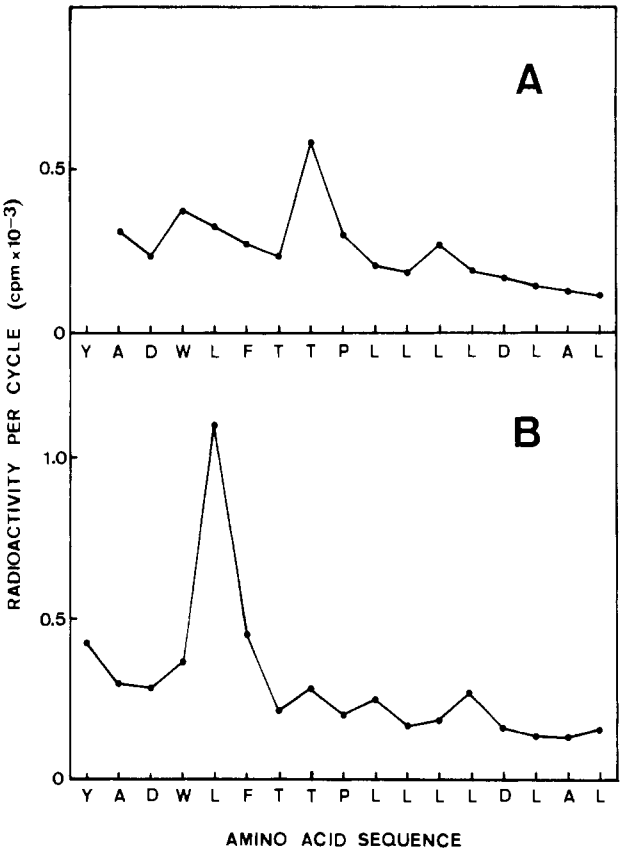

FIGURE 4: Edman degradation of [^{125}I]TID-labeled CNBr 9a fragment. Lyophilized mixtures of labeled and unlabeled CNBr 9a were treated with trifluoroacetic acid (25 °C, 1 h). Dried homoserine lactone activated peptides were then attached to AEAP-glass, and peptide not bound was removed by washing the glass beads with DMF, methanol, formic acid, methanol, 1,2-dichloroethane, and ether. After cleavage of an N-terminal tetradecapeptide with trypsin, the glass beads were washed again as described above, and the remaining glass-bound peptide was sequenced in a Sequemat Mini-15 with the program described (see Experimental Procedures). The radioactivity released at different cycles is plotted and the corresponding amino acid sequence indicated by the one-letter code. Repetitive Edman degradation yields were determined by HPLC analyses of the resultant PTH-amino acids to be approximately 93%. (A) Radioactivity profile obtained from sequencing of [^{125}I]TID-labeled CNBr 9a fragment from pool A (see text); (B) radioactivity profile obtained from sequencing of [^{125}I]TID-labeled CNBr 9a fragment from pool B (see text). The input radioactivities were 13.3 × 10^3 cpm (A) and 21.3 × 10^3 cpm (B).

peaks in the profiles reflect the major sites of [^{125}I]TID labeling within the amino acid sequence. In all degradation experiments performed, we noticed the release of some radioactivity at each cycle, which is likely to be due to some leaching out of peptide from the glass as a result of slow hydrolysis of the N-acylhomoserinamide bond under the conditions of Edman degradation.

The radioactivity profiles clearly demonstrate that pool A and pool B peptides differed in both sites and extents of modifications. Thus, pool A material appears to be labeled at Trp$_4$, Leu$_5$, Thr$_8$, and Leu$_{12}$ whereas the major sites of labeling of pool B peptide were Leu$_5$, Thr$_8$, Leu$_{10}$, and Leu$_{13}$. When peptides from pools A and B combined were sequenced, the resulting radioactivity pattern showed close similarities with the superimposed profiles obtained from degradations of the indivudal pools (data not shown). Furthermore, in spite of the limitations of this method in assigning label to individual amino acid residues, qualitatively the same results were obtained from three other, completely independent, labeling and degradation experiments.

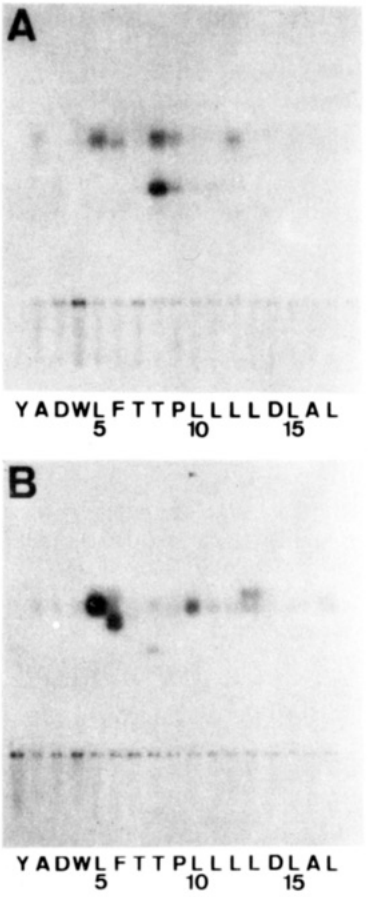

FIGURE 5: Autoradiogram demonstrating the TLC patterns of the radioactive derivatives of PTH-amino acids as obtained from Edman degradations depicted in Figure 4. After conversion of the anilinothiazolinones into PTH-amino acid, these were dissolved in 10 μL of acetonitrile, and 3-μL aliquots each were applied onto HPTLC silica gel plates (Merck). Chloroform–ethanol (98:2 v/v) was used to develop the chromatograms, which subsequently were exposed to Kodak X-0-mat films at −80 °C for 1 week. (A) PTH-amino acid derivatives from sequencing of [^{125}I]TID-labeled CNBr 9a fragment from pool A (see text); (B) PTH-amino acid derivatives obtained from sequencing of [^{125}I]TID-labeled CNBr 9a fragment from pool B (see text).

Following Edman sequencing, individual [^{125}I]TID-labeled derivatives of PTH-amino acids were analyzed by TLC as described earlier (Hoppe et al., 1984). This procedure permitted a closer examination of the materials actually carrying the label. As suggested by Hoppe et al. (1984), these TLC patterns of the radioactive components are quite characteristic, or even unique, for a given amino acid residue. Consequently, it is also possible to identify the corresponding amino acid from such a pattern and, thereby, provide critical information concerning the sequence of the labeled peptide. For example, the pattern obtained at cycle 6 (Figure 5B) is indistinguishable from the "Phe" pattern resulting at cycle 20 on sequencing of [^{125}I]TID-labeled light-harvesting protein from *R. rubrum* (data not shown). On the other hand, it is distinctly different from the patterns obtained at all other cycles not corresponding to Phe. Thus, this procedure allowed the unambiguous identification of a Phe at position 6 in the sequence, which is only compatible with the labeled peptide being derived from CNBr 9a (any other possibility can be excluded on the basis of the bR sequence). Unfortunately, due to lack of corresponding reference patterns, it has not yet been possible to make similar comparisons with the heavily labeled residue at position 8 (presumed to be Thr) of pool A peptide (Figure 5A). However, there is a good agreement in the radioactivity patterns obtained at degradation steps predicted to correspond to the various labeled leucines (Leu_5, Leu_{10}, Leu_{12}, Leu_{13}, and Leu_{17}).[2] Thus, in addition to demonstrating that the radioactive components in pools A and B (Figure 2) had the same electrophoretic mobilities as unlabeled CNBr 9a, with this analysis, we have also shown an agreement in their amino acid sequences.

In addition, the autoradiographs (Figure 5) suggest that the radioactivity released at cycle 6 of peptide from pool A was likely to be due to some "carry-over" from the preceding strongly labeled Leu (same pattern) whereas it was at least partially due to labeled Phe in the case of pool B peptide (different patterns). As to Trp_4, TLC analysis (Figure 5A) did not substantiate labeling of these residue as was suggested by the radioactivity elution profile (Figure 4A). It seems more likely that the radioactivity eluted at that cycle was (mainly) due to an increased level of peptide liberated from the glass [the radioactivity remained at the start (Figure 5A), which is diagnostic for charged residues or entire peptides (Hoppe et al., 1984)]. On the other hand, although not unequivocally evident from the radioactivity elution profile (Figure 4B), the TLC analysis consistently suggested some labeling of Leu_{17}. The small amount of radioactivity released at that cycle gave a pattern that is characteristic for that of [^{125}I]TID-labeled PTH-Leu. Finally, the data of Figures 4 and 5 indicate that some labeling may have occurred also at Ala_2. From the present analysis we conclude that the following residues of helix C were labeled by [^{125}I]TID: (Ala_2), Leu_5, Phe_6, Thr_8, Leu_{10}, Leu_{12}, Leu_{13}, and Leu_{17}.

Stability of Esters Derived from Carbene Insertion into Carboxyl Groups. Interpretation of labeling results should consider the possible chemical instabilities of some of the putative products formed. In this work, the apparent absence of label in Asp_3 and Asp_{14} (Figure 4) was of particular interest. This could have been the result of a true inaccessibility of these sites to the carbene or else that of a limited stability (and thus breakdown) of the ester, and likely insertion product formed. By considering the harsh conditions used for protein fragmentation (70% aqueous formic acid) or for fragment separation (formic acid–ethanol), the latter possibility seemed a quite reasonable one. To examine this point, we have synthesized the model compound (I) and measured the rates at

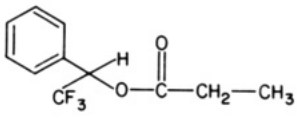

I

which it was hydrolyzed or transesterfied in formic acid, in formic acid–ethanol, or in 1.5 M methanolic HCl.

The main results of these experiments were that ester I was perfectly stable in formic acid or formic acid–ethanol (up to 48 h at room temperature) whereas it was cleaved (half-time approximately 2 h) in methanolic HCl. Therefore, these results imply that in fact the two Asp residues mentioned had not been labeled by [^{125}I]TID in spite of the predicted high intrinsic reactivity of the carboxyl group toward the carbene. Examination of the stability of ester I in methanolic HCl was recommended by the fact that prior to sequencing of many

[2] In all experiments performed, we noticed that the thin-layer chromatographic pattern of the [^{125}I]TID-labeled derivatives of PTH-Leu released at cycle 13 differed somewhat from those obtained at cycles 5, 10, 12, and 17. This could be due to different points of insertion of the carbene into the side chain of Leu_{13} when compared with the other leucines. Alternatively, it could reflect a diastereomeric effect.

proteins a deformylation of the N-terminus is required, which is generally carried out by treatment of the protein with methanolic HCl. From the present data, it is clear that such treatment would result in a substantial loss of that fraction of the photolabel bound to side-chain carboxyl groups of Asp and Glu.

Discussion

Methodological Aspects. Earlier [^{125}I]TID-labeling studies, and notably that with F_1F_0 ATP synthase complex from *E. coli* (Hoppe et al., 1984), strongly suggest that detailed analyses of the labeling patterns can provide important structural and topological information. However, it also became clear that the available methodology cannot be applied to large membrane-embedded proteins without further evaluations concerning the preparation of [^{125}I]TID-labeled fragments from such proteins.

Unlike the modification of proteins with conventional reagents exhibiting high chemical selectivity, [^{125}I]TID labeling leads to a host of products with undefined stoichiometry. Furthermore, as suggested by Hoppe et al. (1984), reactions at methionyl side chains prevents subsequent cleavage at these sites by CNBr and more complex fragmentation patterns result. On the other hand, additional sites for peptide cleavage may be generated upon reaction of the carbene with the polypeptide backbone. These reactions are presumed to yield imido ester (White et al., 1978) which are highly susceptible to acid hydrolysis.

In the present study, CNBr fragments of [^{125}I]TID-labeled bR were first fractionated according to size by Sephadex LH-60 gel filtration in ethanol–formic acid. As shown by subsequent NaDodSO$_4$–polacrylamide gel electrophoretic analyses, the labeled and unlabled CNBr 9a coeluted from this column, which is in agreement with results of a similar study with peptides labeled with sprio[adamantane-4,3′-diazirine] (Nicholas, 1984). Final purification of the [^{125}I]TID-labeled peptide was then achieved by reverse-phase HPLC in essentially the system devised by Khorana and co-workers (Gerber et al., 1979; Takagaki et al., 1980). However, because upon labeling with [^{125}I]TID some of the CNBr 9a no longer coluted with the unlabeled peptide, additional efforts were necessary to ensure quantitative recovery of the labeled peptide. As became evident from these analyses, about half of the labeled peptide eluted as a broad peak, indicating inhomogeneous labeling by [^{125}I]TID. Its position in the elution profile was further indicative of a material that is more hydrophobic than the unlabeled CNBr 9a or the coeluting [^{125}I]TID-labled counterpart.

Although the major sites of [^{125}I]TID-labeling (within the segment sequenced) are now known, we cannot offer a final explanation for the appearance of [^{125}I]TID-labeled CNBr 9a within two distinct pools. However, it is very unlikely that it reflects different extents of labeling. In fact, even at the highest reagent concentration used in experiments with subsequent isolation of [^{125}I]TID-labeled CNBr 9a, less than 0.3 molecule of photolabel was incorporated per molecule of bR. This ratio is much smaller even when CNBr 9a is considered (0.06 molecule of label per copy of peptide), which suggests that virtually all of the labeled CNBr 9a molecules contained a single reagent residue. On the basis of such considerations, one might assume that pool A and pool B peptides should not have common sites of labeling (why should labeling of the same sites give rise to products exhibiting different chromatographic propertes?). A possible and most trivial answer is that there were cross-contaminations due to incomplete separation of pool A and pool B peptides. Al alternative explanation considers the fact that carbene insertion into a given amino acid residue can give rise to more than one product, which may differ in their properties. For example, most aliphatic side chains contain primary, secondary, and tertiary C–H bonds with different and varying reactivities and accessibilities, respectively. Futhermore, one should also consider that insertion of the carbene into a single bond (C–H, O–H, etc.) generates at least one additional chiral center (at the carbene carbon). In the case of modified amino acids and peptides, this results in diastereomers, which, in principle, exhibit different chromatographic properties. Heterogeneous behavior of photolabeled peptides on HPLC is, therefore, not unexpected, and the present work reveals just another aspect of a general problem that has been addressed recently by Nicholas (1984).

Unambiguous identification of the [^{125}I]TID-labeled CNBr 9a represented another critical step in this study. First, evidence that pool A and B (Figure 2) contained the desired fragment came from NaDodSO$_4$–polyacrylamide gel electrophoretic analysis, which revealed mobilities of the radioactive component(s) indistinguishable from that of unlabeled CNBr 9a. Since this procedure separates polypeptides as a function of chain length, it was to be expected that the electrophoretic mobilities would not be markedly affected by the covalent additon of a single photolabel group. However, we wish to point to another labeling study in which slight shifts toward higher molecular weight were observed for two proteins, the β-subunit (M_r 11 000) and the γ-subunit (M_r 9000) of cholera toxin, following labeling with a phospholipid analogue (Tomasi & Montecucco, 1981). Final identification of the [^{125}I]TID-labeled CNBr 9a was then based on TLC analyses of the radioactive PTH-amino acid derivatives following Edman sequencing of the peptides. Clearly, further work is needed to establish the TLC patterns for all [^{125}I]TID-labeled PTH-amino acids and to define variations that may result from labeling of a given residue in different environments. Nonetheless, it is clear that the method pursued here should be applicable to the identification of other [^{125}I]TID-labeled peptides as well.

In cases in which [^{125}I]TID-labeled peptides exhibit heterogeneity, quantitative recovery of peptides on the one hand, and an analysis representative of the entire population of peptides on the other, became critical requirements for the present work. With respect to the former point, we have shown by NaDodSO$_4$–polyacrylamide gel electrophoresis that the radioactive peptides comigrating with CNBr 9a were all contained within pools A and B. For the latter requirement, we demonstrated that coupling to glass of [^{125}I]TID-labeled peptides from pools A and B was not affected by the [^{125}I]TID modification. In fact, the coupling efficiencies for peptides from both pools were as for the nonlabeled CNBr 9a, which reduces the possibility that Edman degradation had been performed on a subpopulation of [^{125}I]TID-labeled CNBr 9a that did bind preferentially to glass.

The Edman sequencing results provide further evidence that the carbene generated from [^{125}I]TID reacted with aliphatic side chains accessible. Although we do not yet know the structure of the covalent adducts formed, it is reasonable to assume that most of them arose from insertion of the carbene into C–H bonds, preferentially into tertiary C–H bonds. It is very possible that these reactions are favored in the viscous and highly anisotropic medium of a biological membrane. Attack of the carbene generated from TID on the peptide carbonyl group has not yet been demonstrated, but as indicated by model studies of White et al. (1978), this would presumably result in the formation of imido esters and in cleavage of the

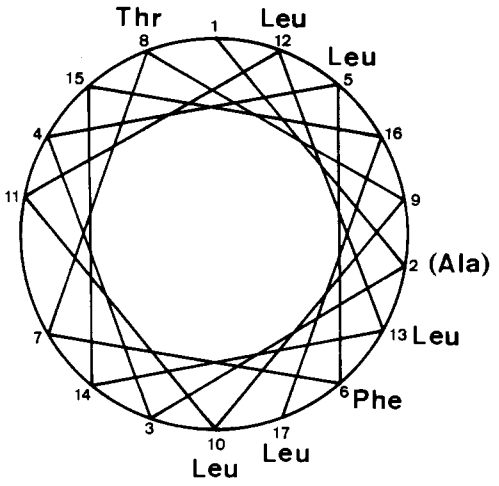

FIGURE 6: Axial projection of helix C (see text) of bR depicting the main sites of labeling with [^{125}I]TID by the three-letter code of the corresponding amino acids.

peptide at the points of carbene insertion in the course of subsequent acid treatments. An aspect investigated in this study concerns the stability of the putative esters formed by attack of a side-chain carboxyl group by the carbene. Our data with the model compound 2,2,2-trifluoro-1-phenylethyl propionate strongly suggest that neither ester hydrolysis nor transesterification reactions occur under conditions that were used for protein fragmentation and fragment purification. However, as suggested earlier (Hoppe et al., 1984) and confirmed here, treatment of the ester with methanolic HCl causes a relatively rapid cleavage of the 2,2,2-trifluoro-1-phenylethyl ester group.

Interpretation of [^{125}I]TID-Labeling Results. Labeling of integral proteins with [^{125}I]TID was shown previously to be confined to membranous segments of integral proteins (Brunner & Semenza, 1981; Spiess et al., 1982). Therefore, we conclude that the region in CNBr 9a labeled with [^{125}I]TID corresponds to a segment in the native protein that is buried in the membrane. According to the model of Henderson & Unwin (1975), bR consists of seven, closely packed, α-helical segments that cross the bilayer roughly perpendicular to the plane of the membrane. Although alternative models, e.g., one consisting of five α-helices and four strands of β-sheet (Jap et al. 1983), were also considered for bR, recent neutron diffraction data are consistent with the segment analyzed here being (part of) a transmembrane helical rod of which one face only is exposed to the bilayer (Trewhella et al., 1983). Assuming that labeling exclusively occurred at residues that make direct contact with the lipids, the topology of this putative "sided" helix was expected to be reflected in the distribution of labeled sites along the polypeptide chain. Figure 6 suggests such a correlation in that seven out of eight residues labeled are located on one face of a cylinder circumscribing a helix with 3.6 residues per turn of the polypeptide coil. This face may correspond to that side of the helix that is oriented toward the outside, the lipid bilayer, of the bR molecule. It should be clear, however, that more structural details are needed to confirm the validity of this model.

Two features of the labeling pattern deserve further comments: First, since the extent of labeling of a given residue is a function of both reagent accessibility and intrinsic reactivity of that residue, it would be particularly informative to analyze the label distribution among identical residues. The extraordinarily high content of leucines (7 out of 17 residues sequenced) provided such an opportunity (and made such a comparison meaingful). As shown in Figure 6, five of these residues were labeled and two of them were not. Interestingly, the distribution of these residues is again as predicted: all labeled Leu are on the one half of the cylinder whereas the two unlabeled ones (Leu_{11} and Leu_{15}) are on the opposite half. Second, within the segment analyzed, four residues have polar (Thr_7 and Thr_8) or charged (Asp_3 and Asp_{14}) side chains. Three of them (Asp_3, Thr_7, and Asp_{14}) were not detectably labeled. These unlabeled residues also lie within a narrow section in the cylinder projection, which according to the present model would face the inside of the protein. This agrees with the conclusion by Engelman & Zaccai (1980) suggesting that, unlike soluble proteins, bR is an "inside-out" protein in which polar and charged residues tend to lie at the interior of the molecule (where they may participate in proton conduction).

Though noting some difficulties in purifying and analyzing [^{125}I]TID-labeled CNBr 9a, the main conclusion of this work is that this type of carbene-generating reagents represents promising probes for various aspects of membrane structure and dynamics. Specifically, it may be possible to determine and map protein–lipid interfaces of integral proteins at a high level of resolution.

ACKNOWLEDGMENTS

We thank Prof. Winterhalter for the opportunity to utilize the sequencing facilities in his laboratory and Markus Rimle for help in measuring partition coefficients.

Registry No. Thr, 72-19-5; Leu, 61-90-5; Ala, 56-41-7; Phe, 63-91-2; [^{125}I]TID, 79684-41-6; 2,2,2-trifluoracetophenone, 434-45-7; 2,2,2-trifluoro-1-phenylethanol, 340-04-5; 2,2,2-trifluoro-1-phenylethyl propionate, 97732-37-1.

REFERENCES

Bayley, H. (1983) in *Photogenerated Reagents in Biochemistry and Molecular Biology* (Work, T. S., & Burdon, R. H., Eds.) Elsevier, Amsterdam.

Bayley, H., & Knowles, J. R. (1978a) *Biochemistry 17*, 2414–2419.

Bayley, H., & Knowles, J. R. (1978b) *Biochemistry 17*, 2420–2423.

Bercovici, T., & Gitler, C. (1978) *Biochemistry 17*, 1484–1489.

Brunner, J. (1981) *Trends Biochem. Sci. (Pers. Ed.) 6*, 44–46.

Brunner, J., & Richards, F. M. (1980) *J. Biol. Chem. 255*, 3319–3329.

Brunner, J., & Semenza, G. (1981) *Biochemistry 20*, 7174–7182.

Brunner, J., Spiess, M., Aggeler, R., Huber, P., & Semenza, G. (1983) *Biochemistry 22*, 3812–3820.

Chakrabarti, P., & Khorana, H. B. (1975) *Biochemistry 14*, 5021–5033.

Engelman, D. M., & Zaccai, G. (1980) *Proc. Natl. Acad. Sci. U.S.A. 77*, 5894–5898.

Gerber, G. E., & Khorana, H. G. (1982) *Methods Enzymol. 88*, 56–74.

Gerber, G. E., Anderegg, R. J., Herlihy, W. C., Gray, C. P., Biemann, K., & Khorana, H. G. (1979) *Proc. Natl. Acad. Sci. U.S.A. 76*, 227–231.

Gupta, C. M., Radhakrishnan, R., Gerber, G. E., Olsen, W. L., Quay, S. C., & Khorana, H. G. (1979) *Proc. Natl. Acad. Sci. U.S.A. 76*, 2595–2599.

Henderson, R., & Unwin, P. N. T. (1975) *Nature (London) 257*, 28–32.

Hoppe, J., & Sebald, W. (1984) in *H^+-ATPsynthases* (Papa, S., Altendorf, K. H., Ernster, L., & Packer, L., Eds.) pp

173–180, JCSU Press, Bari, Italy.
Hoppe, J., Brunner, J., & Jørgensen, B. B. (1984) *Biochemistry 23*, 5610–5616.
Jap, B. K., Maestre, M. F., Hayward, S. B., & Glaeser, R. M. (1983) *Biophys. J. 43*, 81–89.
Khorana, H. G., Gerber, G. E., Herlihy, W. C., Gray, C. P., Anderegg, R. J., Nihei, K., & Biemann, K. (1979) *Proc. Natl. Acad. Sci. U.S.A. 76*, 5046–5050.
Klip, A., & Gitler, C. (1974) *Biochem. Biophys. Res. Commun. 60*, 1155–1162.
Lämmli, U. K. (1970) *Nature (London) 227*, 680–685.
Nicholas, R. A. (1984) *Biochemistry 23*, 888–898.
Oesterhelt, D., & Stoeckenius, W. (1974) *Methods Enzymol. 31*, 667–678.
Peters, H. M., Feigl, D. M., & Mosher, H. S. (1968) *J. Org. Chem. 33*, 4245–4250.
Ross, A., Radhakrishnan, R., Robson, R. J., & Khorana, H. G. (1982) *J. Biol. Chem. 257*, 4152–4161.
Shapiro, A. L., Viñuela, E., & Maizel, J. B. (1967) *Biochem. Biophys. Res. Commun. 28*, 815–820.
Spiess, M., Brunner, J., & Semenza, G. (1982) *J. Biol. Chem. 257*, 2370–2377.
Stoeckenius, W. (1980) *Acc. Chem. Res. 13*, 337–344.
Takagaki, Y., Gerber, G. E., Nihei, K., & Khorana, H. G. (1980) *J. Biol. Chem. 255*, 1536–1541.
Takagaki, Y., Radhakrishnan, R., Gupta, C. M., & Khorana, H. G. (1983a) *J. Biol. Chem. 258*, 9128–9135.
Takagaki, Y., Radhakrishnan, R., Wirtz, K. W. A., & Khorana, H. G. (1983b) *J. Biol. Chem. 258*, 9136–9142.
Tomasi, M., & Montecucco, C. (1981) *J. Biol. Chem. 256*, 11177–11181.
Trewhella, J., Anderson, S., Fox, R., Gogol, E., Khan, S., Engelman, D., & Zaccai, G. (1983) *Biophys. J. 42*, 233–241.
White, E. H., Perks, H. M., & Roswell, D. F. (1978) *J. Am. Chem. Soc. 100*, 7421–7423.

Thiol-Specific Probes Indicate That the β-Chain of Platelet Glycoprotein Ib Is a Transmembrane Protein with a Reactive Endofacial Sulfhydryl Group†

Efstathia L. Kalomiris‡ and Barry S. Coller*

Departments of Pathology and Medicine, State University of New York at Stony Brook, Stony Brook, New York 11794

Received January 7, 1985

ABSTRACT: We used two membrane-permeable fluorescent reagents, monobromobimane and *N*-[[5-(dimethylamino)-1-naphthalenyl]sulfonyl]aziridine (*N*-dansylaziridine), and one membrane-impermeable fluorescent probe, monobromo(trimethylammonio)bimane, all three of which react selectively with protein thiols, to (1) assess the presence of reactive sulfhydryls in the platelet glycoprotein Ib (GPIb) molecule and (2) establish the topology of any GPIb-reactive thiols in the platelet membrane. Intact platelets were reacted with 1–10 mM monobromobimane or monobromo(trimethylammonio)bimane or 50–100 μM *N*-dansylaziridine for 30–60 min at 37 °C. The platelets were then washed, solubilized in 1% Triton X-100, and analyzed by nonreduced–reduced polyacrylamide gel electrophoresis either directly or indirectly after immunopurification of GPIb. Monobromobimane and *N*-dansylaziridine labeled GPIbβ but not GPIbα in intact platelets. This labeling could be inhibited by pretreating the platelets with either *N*-ethylmaleimide or *p*-(chloromercuri)benzenesulfonic acid, confirming the specificity of these probes for thiol groups. Monobromo(trimethylammonio)bimane, the membrane-impermeable reagent, did not label GPIbβ in intact platelets. However, it did label GPIbβ in sonicated platelets, indicating that the thiol group of GPIbβ occupies an intracellular location. Since the carbohydrate moiety of GPIbβ can be labeled from the outside of intact platelets with membrane-impermeable reagents, we conclude that GPIbβ has a transmembrane orientation.

The mechanism(s) by which platelet membrane events affect intracytoplasmic constituents and the way(s) in which intracytoplasmic constituents modulate platelet membrane events are the subject of intense study. Much work has focused on changes in lipids, calcium, and cyclic nucleotides as transducing agents (Holmsen & Karpatkin, 1983; Lasslo & Quintana, 1984) with growing evidence that a dynamic structural interaction exists between membrane glycoproteins and the cytoskeletal proteins contained within the cytoplasm (Phillips et al., 1980). There is circumstantial evidence to suspect that protein sulfhydryl and disulfide groups may be contributing to these processes since (1) sulfhydryl blocking agents are powerful inhibitors of platelet phospholipid metabolism and platelet aggregation (Harbury & Schrier, 1974; MacIntyre et al., 1977; Silk et al., 1981), (2) platelets can be aggregated by the disulfide reducing agent dithiothreitol (Zucker et al., 1983), (3) the sulfhydryl oxidizing agent diamide induces aggregate formation of cytoskeletal proteins, inhibits the induction of platelet aggregation, and promotes the deaggregation of previously aggregated platelets (Ando & Steiner,

† This investigation was supported, in part, by Grant 19278 from the National Heart, Lung, and Blood Institute, by a grant-in-aid from the American Heart Association, and with funds contributed in part by the American Heart Association, Suffolk County Chapter, NY.

* Address correspondence and reprint requests to this author at the Division of Hematology, State University of New York at Stony Brook, Stony Brook, NY 11794.

‡ This paper contains work performed by E.L.K. in partial fulfillment of the Ph.D. degree in Experimental Pathology. Present address: Department of Medicine (R-38), University of Miami School of Medicine, Miami, FL 33101.

0006-2960/85/0424-5430$01.50/0